Correct stimulation of CD28H arms NK cells against tumor cells

Raphaëlle Leau, Pierre Duplouye, Virginie Huchet, Véronique Nerrière-Daguin, Bernard Martinet, Mélanie Néel, Martin Morin, Richard Danger, Cécile Braudeau, Régis Josien, et al.

Correct stimulation of CD28H arms NK cells against tumor cells

Fabienne HASPOT (fabienne.haspot@univ-nantes.fr)
Nantes Université
Pierre Duplouye
CHU Nantes
Raphaëlle Leau
Nantes Université
Virgnie Huchet
Nantes Université
Véronique Nerrière-Daguin
Nantes Université
Bernard Martinet
Nantes Université
Richard Danger
CRTI, UMR1064, INSERM, Université de Nantes
Cécile Braudeau
CHU NANTES
Régis Josien
Nantes Université
Gilles Blancho
Nantes Université

Article

Keywords:

Posted Date: October 12th, 2023

DOI: https://doi.org/10.21203/rs.3.rs-3408654/v1

Additional Declarations:
(Not answered)

Table 1 is available in the Supplementary Files section.

Correct stimulation of CD28H arms NK cells against tumor cells

Pierre Duplouye[1], Raphaëlle Leau[1], Virginie Huchet[1], Véronique Nerrière-Daguin[1], Bernard Martinet[1], Richard Danger[1], Cécile Braudeau[1, 2], Régis Josien[1, 2], Gilles Blancho[1] and Fabienne Haspot[1]

[1] Nantes Université, CHU Nantes, INSERM, Center for Research in Transplantation and Translational Immunology, UMR 1064, ITUN, F-44000, Nantes, France
[2] CHU Nantes, Laboratoire d'Immunologie, CIMNA, F-44000 Nantes, France

Running title: Specific anti-CD28H mAb activates NK cells

Corresponding author :

Fabienne HASPOT, CR2TI, 30 Bd Jean Monnet, 44093 Nantes, France,

+33(0)2 40 08 75 87 fabienne.haspot@univ-nantes.fr

Abstract

Tumor evasion has recently been associated with a new member of the B7 family, HHLA2, mostly overexpressed on PDL1^{neg} tumors. HHLA2 can either induce a costimulation signal when binding to CD28H or inhibition by binding to KIR3DL3 on T and NK cells. Given the broad distribution of CD28H on NK cells and its depicted role, we compare in this study two monoclonal antibodies targeting this new NK cell engager. We show that targeting CD28H at a specific epitope not only strongly activates Ca^{2+} flux but also results in NK cell activation. CD28H-activated NK cells further display increased cytotoxic activities against hematopoietic cell lines and bypass HHLA2 and HLA-E inhibitory signals. Additionally, scRNASeq analysis of clear cell kidney cancer cells (ccRCC) reveals that HHLA2^{+} ccRCC tumors are infiltrated with CD28H^{+}NK cells which thus could be targeted by finely chosen anti-CD28H Abs.

Introduction

Immune checkpoint inhibitors (ICI) of the B7 family e.g., anti-CTLA4, anti-PD1 and anti-PDL1 have revolutionized oncotherapy in recent decades. Yet, some patients face primary or secondary resistance to ICI treatment, suggesting that tumor complexity and heterogeneity between and among patients needs to be considered. A new member of the B7 family, HHLA2 (HERV-H LTR-associating 2), has recently been discovered in humans, but its absence in rodents has made it difficult to study.

HHLA2 was originally described to be expressed by epithelial cells of the colon, the kidney, the small intestine, and the lung (1,2) and to be elevated notably in renal cancers (3). Interestingly, it has been shown that clear cell kidney cancer cells (ccRCC) express either HHLA2 or PDL1 but rarely both, in which case HHLA2+ and PDL1+ expressions were not overlapping (4). Like B7-1 and B7-2, HHLA2 has two ligands on immune cells: CD28H (also known as IGPR1 or TMIGD2) is the activating receptor (5,6), while KIR3DL3 is the inhibitory one (4,7). CD28H is expressed on T cells, NK cells, ILCs, and pDC (5,8) and it binds to HHLA2's IgV1 domain (7). Demonstrating KIR3DL3 protein expression on T and NK cells is challenging due to its poor to no expression on circulating T and NK cells (4,9) and to difficulties in obtaining reliable antibodies because of homologies between the KIR proteins (4,7,9,10). However, KIR3DL3 is detected on some modified NK92 cells (i.e., NK92-MI) (4,7). Interestingly, KIR3DL3 and CD28H can simultaneously bind HHLA2 at different epitopes (7). Several antibodies with inhibitory or activator functions have been developed to target this new tryptic (4,5,7,11) and CD28H-extracellular portion has been used to develop CAR-NK cells (6,12).

Considering the broad distribution of CD28H on NK cells and its depicted role, we hypothesized that anti-CD28H immunotherapy would boost their functions. This strategy would be advantageous as compared to recently described CD28H-CAR-NKL whose action will be restricted to $HHLA2^{pos}$ tumor cells. In this study, we compare two anti-CD28H monoclonal antibodies (mAbs) and demonstrate that targeting CD28H at the correct epitope not only strongly activates Ca^{2+} flux but also results in NK cell activation. CD28H-activated NK cells further display increased cytotoxic activity against hematopoietic cell lines and bypass HHLA2

and HLA-E inhibitory abilities. Finally, single-cell RNA sequencing (scRNASeq) analysis of 16 primary ccRCC (13) reveals that HHLA2^{+} ccRCC tumors are infiltrated by CD28H^{+}KIR3DL3^{neg} NK cells which could be targeted by finely selected anti-CD28H Abs.

Materials and methods

Key resources

Material used in this study has been listed in the Table I.

Cells

Human peripheral blood mononuclear cells (PBMC) were isolated from blood collected at the Etablissement Français du Sang (EFS, Nantes, France) from healthy donors (HD) with written informed consent. NK cells were isolated by a negative selection with the Miltenyi's NK cell isolation kit, purity was analyzed by flow cytometry staining on $CD56^{+}CD3^{neg}$ and reach 90,64% ± 4% (Supplementary Figure 1A). Purified NK cells were cultured overnight (overnight) at 37°C (5% C02) in complete medium (RPMI, Gibco®), 10% Fetal Bovine Serum (GE Healthcare HyClone™), 1% Penicillin-Streptomycin (Gibco®, 1% Glutamine) supplemented with 10 UI rhIL-2 (Cellgenix) with indicated mAbs at 10□g/ml. Tumor cell lines K562 (ATCC® CCL-243™), DAUDI (ATCC® CCL-213™), and JURKAT were cultivated in complete medium. The K562-$HHLA2^{+}$ cells were developed in our laboratory by cloning the HHLA2 sequence (NP_009003) (synthesized by Genscript) into the pHIV-Luciferase (Addgene plasmid #21375). Transduced-K562 cells were FACS-sorted according to their HHLA2 expression. K562 HLA-A*02 and K562 HLA-A*02 HLA-E cells were a gift of Dr L. Vidard (Sanofi, Virty sur Seine, France).

Characterization of the two anti-CD28H mAbs by Bio-Layer Interferometry

The CD28H-HHLA2 interaction in the presence of the anti-CD28H mAbs (clones 4-5 and MAB83162 from R&D) has been evaluated by Bio-Layer Interferometry BLItz® System (Fortebio). First, the TMIGD2/CD28H His-tag recombinant protein (R&D) was loaded on an anti-HIS biosensors, after a wash with a specific Fortebio buffer. The biosensor was plunged in a 10□g/ml anti-CD28H (clone 4-5 or MAB83162) solution. The biosensor was further washed prior to being plunged in a solution containing the HHLA-2-Ig recombinant molecule (R&D).

Production of the anti-CD28H monoclonal antibody clone 4-5

The hybridoma allowing the production of the hamster anti-human CD28H monoclonal antibody (mAb) (clone 4-5), generously provided by Dr Lieping Cheng (5), was cultured in

IMDM with 10% FBS. Antibodies in supernatant were purified by Hitrap protein G affinity column (GE Healthcare).

Calcium flux

One million NK cells were incubated with 5 µM of Fura Red™ in calcium-free HBSS for 30 min at 37°C. NK cells were then incubated on ice for 30 min with primary antibodies. Cells were resuspended in HBSS supplemented with 10 mM HEPES, 1% BSA, 1 mM $CaCl_2$, and were acquired during 45 sec with the FACS Celesta (BD Biosciences) prior to the addition of a cross-linker mix to induce calcium flow. The cross-linker mix was composed of 4□g of the anti-Armenian hamster and 4□g of the goat anti–mouse F(ab')2 antibodies (Table 1). Once cross-linked, samples were vortexed and acquired on the FACS Celesta.

Staining procedure and flow cytometry assays

Cells ($5x10^5$ per well) suspended in 200µL of FACS buffer (Phosphate buffer Saline 1X, 1% Bovine serum albumin Sigma-Aldrich, 0,1% Azide Sigma-Aldrich) were plated in a V-bottom 96-well plate prior to centrifugation at 2500 rpm 1 min. For extracellular staining, antibodies were added to each well and the cells were incubated for 30 minutes on ice in the dark. For intracellular labeling, Brefeldin A (5□g/ml final) was added to the cell culture (i.e., NK □ K562) during 4h prior to the use of the BD Cytofix/Cytoperm kit accordingly to the manufacturer's protocol with recommended volume of intracellular antibodies (anti-IFNγ). Finally, the cells were washed twice before fluorescence acquisition with a FACS Celesta or an LSRII (BD Bioscience). Results were analyzed with FlowJo software (Tree Star, Ashland, OR). For receptor/ligand interaction, recombinant proteins were used at 5□g/ml and added on the cells for 1h at 37°C, after two washes, cells were stained with anti-Human-Fc secondary Ab for 30 min on ice in the dark.

RNA Seq preparation and analysis

Isolated NK cells were incubated overnight in complete RPMI medium supplemented with 10 UI rhIL-2 and stimulated or not with 10□g/ml of anti-CD28H (clone 4/5) or the isotype control. Sixteen hours later, 2 million NK cells from each condition were washed in PBS and the dry pellet was frozen at -80°C. Samples were then sent to QIAGEN Genomic Services

(Germany) for RNA extraction, library preparation, sequencing and reads alignment. Briefly, total RNA extraction was performed using the RNeasy Mini kit (Qiagen) following the manufacturer's protocol. RNA quality was assessed using an Agilent TapeStation 4200 (Agilent Technologies, Santa Clara, CA, USA) and only samples with high RNA integrity values were analyzed (RIN median = 8.1). The library preparation was done using TruSeq Stranded mRNA Sample preparation kit (Illumina inc) with 250 ng of total RNA. Enriched mRNAs using oligodT beads were fragmented using enzymatic fragmentation and used for cDNA synthesis before double stranded cDNA were purified (AMPure XP, Beckman Coulter). The cDNA was end-repaired, 3' adenylated and Illumina sequencing adaptors ligated onto the fragments ends, and the library was purified (AMPure XP). The mRNA stranded libraries were pre-amplified with PCR and purified (AMPure XP). The libraries size distribution was validated, and quality inspected on a BioAnalyzer 4200 tapeStation (Agilent Technologies). Single-end sequencing was carried out on a NextSeq500 instrument (75 cycles) according to the manufacturer instructions (Illumina Inc.). Data were aligned using Tophat (v 2.0.11)(14) and Cufflinks (v2.2.1)(15) with default settings and with the *Homo sapiens* GRCh37 reference genome. On average 43.2 million reads were obtained for each sample and the average genome mapping rate was 96.6%. Differential analysis from transcripts counts was performed using the *edgeR* R package(16). Poorly expressed genes were filtered out by keeping genes with at least 0.5 count per million reads (cpm) in at least half samples. After normalization using trimmed mean of M-values (TMM) method, differential expressed genes were identified using the quasi-likelihood F method. Genes with a Benjamini-Hochberg false-discovery rate (FDR) inferior to 5% and a fold change (FC) superior to 2 were considered significantly differentially expressed. The biological significance of differential genes was assessed using *clusterProfiler* package(17). Gene ontology (GO) categories enriched with an FDR<20% and with at least five genes were selected. The *GOplot* R package was used to represent GO analysis results(18). Redundant GO were reduced and a z-score, corresponding to the number of upregulated genes minus the number of downregulated genes divided by the square root of the number of genes in the category, was calculated. RNA-Seq data can be accessed under GEO accession **n**umber GSE152269.

Cytokine secretion evaluated by Luminex

NK cells were incubated overnight with 10□g/ml of indicated mAbs. The next day, NK cells were washed twice, counted, distributed at the indicated concentration, and incubated with 1x10^6 K562 target cells at 1:1 E:T ratio for 6h. The supernatant was frozen at -80°C. Luminex analysis was performed according to the manufacture's protocol with the Human custom Procartaplex 10 PLEX (PPX-10-MXRWE3N) (Thermofisher).

Calcein cytotoxicity assays

Calcein assays were performed has previously described(19). Briefly, NK cells were cultured overnight in the presence 10□g/ml of indicated mAbs. The next day, NK cells were washed twice, counted, distributed at the indicated concentration. Target cells were incubated with 2 mM of Calcein, washed twice prior to being resuspended at 2x10^5 cells/ml in complete medium containing 10 mM of Probenecid. NK and target cells were incubated for 4h at 37°C (5% C02) with 20,000 labeled tumor cells at different Effector:Target (E:T) ratios. The supernatants transferred into black 96-well black plates (Greiner) were analyzed with at Spark® plate reader (TECAN). Maximum and spontaneous release controls were set up in triplicates using 1% Triton X-100 Sigma-Aldrich or in complete medium, respectively. Specific lysis was calculated as follows:

$$\frac{\text{Test release} - \text{Spontaneous release}}{\text{Maximum release} - \text{Spontaneous release}} \; x \; 100.$$

Processing of published scRNA-seq dataset

The FASTQ files of Alchahin A.M. et al. (2022) (GSE114725) were downloaded. The sequenced 10X libraries were mapped to the GRCh38 human genome using Cell Ranger software (version 7.0.1) with default parameters. The classical pipeline for single cell analysis of Seurat V4.3.0 was used to analyze the raw data from 16 tumor samples, using the following steps (1) Cell selection, (2) filtering, and (3) normalization (with integration correction*).* Data normalization was carried out to remove technical noise and adjust for differences in sequencing depth between samples. Feature selection was performed to identify highly variable genes that drive differences between cell types. Dimensionality reduction was then used to visualize the high-dimensional scRNAseq data in two or three dimensions using Uniform Manifold Approximation and Projection (UMAP). Clustering was then performed to group cells with similar gene expression profiles into discrete cell types. The Louvain graph-based clustering with a 0.5 resolution resulted in 25 clusters (172 143 cells). We selected the NK cell clusters

and used again the classical pipeline for single cell analysis of Seurat V4.3.0 (with integration correction). At the resolution of 0.3, we obtained 8 clusters (28 493 cells).

Statistical analysis

GraphPad was used to perform statistical analysis of the data. *<0.05, **<0.01, ***<0.001, ****<0.0001.

Data sharing statement

All supporting data are available on request from the corre- sponding author.

Results

Targeting CD28H on NK cells with an agonistic mAb induces Ca^{2+} flux and gene regulation

CD28H is highly expressed on T and NK cells (5). To investigate the impact of CD28H triggering on NK cells, we compared two mAbs: one (clone 4-5) obtained from Dr Cheng, known to activate T cells (5), and the other one from R&D Systems, described as blocking the CD28H/HHLA2 interaction. As shown by the Blitz analysis, the anti-CD28H from R&D efficiently blocks HHLA2's binding on CD28H (Figure 1A), while the slight decrease in the HHLA2/CD28H binding observed in the presence of the anti-CD28H clone 4-5 is likely due to steric hindrance (Figure 1A). This suggests that the two mAbs target different epitopes. Activating different NK cell receptors on resting NK cells with mAbs has been shown to differentially mobilize intracellular Ca^{2+} flux (20). Without cross-linking, none of the anti-CD28H mAbs used alone were, by themselves, able to induce a Ca^{2+} flux (Sup Figure 1B). Once cross-linked, the agonistic anti-CD28H induces a strong Ca^{2+} flux while the cross-linking of the blocking anti-CD28H does not (Figure 1B and Sup Figure 1B). Therefore, targeting CD28H with mAbs binding to different epitopes does not induce similar intracellular consequences suggesting that all anti-CD28H mAbs will not act similarly on NK cells. Next, we evaluated each anti-CD28H mAb in pairwise combination with anti-CD16 or anti-NKp46. Indeed, the blocking anti-CD28H mAb has synergistic effect when used together with anti-NKp46 or anti-CD16 in the P815 redirected cytotoxicity assay (6). The anti-CD16 alone induces a small Ca^{2+} flux, which is further increased after cross-linking with a secondary antibody (Sup Figure 1C), confirming published results (20). The overall Ca^{2+} flux induced by the agonistic anti-CD28H was as potent as the one induced by the anti-CD16 or the anti-NKp46 (Figure 1C-D). Co-cross-linking of CD16 and CD28H receptors does not result in a synergistic effect (Figure 1C) while the co-cross-linking of NKp46 and CD28H receptors with the agonistic results in a significant increased Ca^{2+} flux (Figure 1D, Sup Figure 1D). Of note, the co-cross-linking of NKp46 and CD28H with the blocking anti-CD28H did not result in an increase of Ca^{2+} flux as compared to anti-NKp46 alone (Figure 1D). Therefore, the anti-CD28H clone 4-5 is superior to the blocking anti-CD28H in eliciting Ca^{2+} flux upon cross-linking.

Given the strong Ca^{2+} flux observed after CD28H cross-linking with the agonistic mAb, we further investigated the functional consequences of such stimulation. The transcriptional

signature of bulk NK cells was analyzed after an overnight culture with the agonistic anti-CD28H or the isotype control. A comparison of gene expression between these two conditions revealed 216 significantly differentially expressed genes, with 108 upregulated and 108 downregulated (Figure 1E). We analyzed the enrichment of gene ontologies (GOs) related to biological processes associated with these differentially expressed genes in both groups. The GOs in which most of the genes were upregulated include positive regulation of cell adhesion, regulation of immune effector process or lymphocyte activation, positive regulation of external processes and T cell differentiation. On the other hand, GOs in which most of the genes were downregulated comprise leucocyte migration, neutrophil activation, positive regulation of secretion and cytokine production (Figure 1F). Interestingly, *TNFRSF9* (4-1BB), *CRTAM* (21)*, IL2RA* and *IRF4* were highly upregulated, revealing increased-NK cell activation and effector functions upon CD28H triggering (Figure 1G). We also compared the obtained gene signature with previously published NK cell signatures (22,23). While no specific GOs enrichment was associated with the commonly differentiated genes, some genes were associated as particular networks (Supplementary Figure 2A, B). Additionally, we performed FACS analysis to evaluate the expression of activation markers on NK cells cultured overnight with the agonistic anti-CD28H. We observed a decrease in CD16 expression as compared to the isotype control (Figure 1H). NK cell activation is known to result in the shedding of the CD16A by ADAM17 regardless of CD16 engagement during this activation (24). The expression of CD69, Tim-3 (25), and 4-1BB (*TNFRSF9)* were significantly upregulated following the anti-CD28H treatment (Figure 1H), confirming the NK cell activation status observed in the bulk RNAseq data (Figure 1F).

In conclusion, when correctly targeted with mAb, the CD28H receptor alone is contributing to a signal in resting NK cells that results in increased Ca^{2+} mobilization and in the regulation of gene expression profiles suggesting the activation of NK cells.

CD28H-activated human NK cells exhibit increased effector functions

Since results presented in Figure 1 demonstrate that the anti-CD28H mAb clone 4-5 is superior to that of R&D System in activating NK cells, we then concentrated on analyzing NK cell effector functions. NK cells activated overnight with the agonistic anti-CD28H or the isotype control prior to a 4 hours treatment with Brefeldin A were then intracellularly stained with anti-IFN-γ. We observed that CD28H triggering results in a significant increase in IFN-γ^{pos} NK cells as compared to NK cells incubated overnight with the isotype control, confirming that CD28H stimulation activates NK cells (Figure 2A). We then hypothesized that this priming would further lead to increased NK cell functions toward K562 cells, a chronic myelogenous leukemia (CML) cell line which does not express HLA class I. Indeed, primed CD28H-NK cells were more potent in producing IFN-γ than ISO-treated NK cells as presented by the intracellular analysis of IFN-γ^+ producing NK cells (Figure 2B). IFN-γ was also significantly more secreted when analyzed in the supernatant of dedicated experiments after 6 hours co-culture with K562 (Figure 2C). MIP-1a (CCL3) and MIP-1b (CCL4) were significantly more secreted by CD28H-preactivated NK cells as compared to control NK cells after 6 hours culture with K562 target cells (Figure 2C). The secretome of primed-NK cells cocultured with K562 cells also revels higher concentration of cytotoxic molecules such as granzyme A and B, FASL and TRAIL. Of note, the blocking anti-CD28H mAb, when used alone, failed to increase the secretion of such soluble factors (Supplementary Figure 3A). There was no synergistic effect when anti-NKp46 and the agonistic anti-CD28H mAb were used to activate NK cells prior to their co-culture with K562 cells (Supplementary Figure 3B). Altogether, these data suggest that stimulation of CD28H should result in the increase of NK cell natural cytotoxicity against K562 target cells. These results indicate that pretreatment with the agonistic anti-CD28H mAb primes NK cells and leads to the secretion of cytotoxic molecules when primed-NK cells were further co-cultured with target cells.

NK cells kill target cells thought Ca^{2+} dependent release of lytic granules or by secreting cytotoxic molecules like FasL and TRAIL through a Ca^{2+} independent pathway (26). CD28H-triggered NK cells cultured with K562 cells displayed increased cytotoxic potential compared to isotype-treated NK cells, as evidenced by the accumulation of granzymes A and B (GZM) as well as FasL and TRAIL in their supernatant. We then investigated the cytolytic functions of CD28H-activated NK cells in a direct cytotoxic assay with calcein-labeled K562 target cells. An

overnight culture of NK cells with the agonistic anti-CD28H mAb significantly increases their cytotoxicity against K562 target cells as compared to NK cells cultured overnight either alone or with the blocking anti-CD28H mAb (Figure 3A) which is aligned with their secretory function (Supplementary Figure 3A). Importantly, there was no significant difference observed when comparing the cytotoxicity of CD16-activated NK cells to that of CD28H-activated NK cells in all E:T ratios but one (i.e., 10:1) (Figure 3B). Although our results on Ca^{2+} flux indicated a synergistic activity between CD28H and NKp46 (Figure 1D), the secretory function in the presence of K562 cells, does not support this observation (Supplementary Figure 3B). Therefore, we evaluated the consequences of NKp46 and CD28H co-engagement on NK cell direct lysis of K562 targets. While the agonistic anti-CD28H and the anti-NKp46 treated-NK cells have similar elevated cytotoxicity against K562 cells, no synergistic effect was observed with the combo pretreatment (i.e., overnight stimulation with both mAbs) (Figure 3C). Of note, the blocking anti-CD28H mAb did not synergize either with the anti-NKp46 in this direct cytotoxicity assay (Figure 3D).

CD28H-activated NK cells do not only show higher cytotoxicity against K562, but also against DAUDI and Jurkat targets (Supplementary Figure 4). In conclusion, we showed that CD28H-triggered NK cells present increased cytotoxicity functions only when the agonistic anti-CD28H mAb is used.

Targeting CD28H bypasses some inhibitory signaling sensed by NK cells

HHLA2 has dual function depending on the receptor it engages. On one hand, HHLA2 activates T and NK cells when binding to CD28H (5,6). On the other hand, HHLA2 inhibits T cell activation and proliferation upon TCR and CD28 stimulation and suppresses NK cell cytotoxic functions by interacting with its inhibitory receptor recently identified as KIR3DL3 (4,7). KIR3DL3 is a polymorphic molecule barely detectable by FACS (27). After screening various cell lines by RT-qPCR followed by FACS analysis using a polyclonal anti-HHLA2 antibody, we did not find a cell line that naturally expresses HHLA2 at the protein level (Supplementary Figure 5A, B). To investigate HHLA2's inhibitory effects, we transduced K562 cells to express HHLA2 (K562-HHLA2+ cells), which were able to bind CD28H-Fc and KIR3DL3-Fc recombinant proteins (Figure 4A). When we loaded K562-$HHLA2^{+}$ cells with calcein, we noticed an increased passive release of calcein as compared to WT K562 cells which could jeopardize the assay (data not shown). To circumvent this, we used a CD107a staining assay to decipher NK cell degranulation

(28). The results showed that NK cell natural cytotoxicity is significantly decreased when target cells express HHLA2 (Figure 4B-C). Importantly, this inhibition is bypassed by CD28H stimulation since CD28H-stimulated NK cell cytotoxicity is restored to a level comparable to that observed with unmodified K562 WT target cells (Figure 4B-C).

When stably expressed with properly loaded peptides, HLA-E is a key mechanism of tumor resistance against cytotoxicity by NK and CD8 T cells (29). Thus, we took advantage of K562 cells modified to express both HLA-A2 and HLA-E (i.e., stably expressing HLA-E) and their controls K562-HLA-A2 which do not express HLA-E (Figure 4D). Both cell lines similarly react to calcein labeling. As expected, K562-HLA-E^+ cells were significantly less killed by NK cells than their control counterparts. Interestingly, NK cells that were stimulated overnight with the agonistic anti-CD28H mAb restored their cytotoxicity against K562-HLA-E^+ cells to a level equivalent to that observed with unstimulated NK cells against the control target cells (Figure 4E). These results clearly demonstrate that CD28H-triggered NK cells can bypass HHLA2 and HLA-E inhibitory signals, indicating that this strategy could still be efficient when targeting $HHLA2^+$ or HLA-E^+ tumor cells, making the use of agonistic anti-CD28h mAb a potential therapeutic approach in such cases.

Single-cell RNA sequencing of primary clear cell renal cell carcinoma (ccRCC) has unveiled the gene expression of CD28H (*TMIGD2*) in a specific $CD56^{bright}$ NK cell cluster

HHLA2 has been shown to be overexpressed in multiple tumor types through transcriptomic analysis and has been identified as an independent prognostic factor in 9 out of 20 human cancers in a pan-cancer survival analysis, especially in renal clear cell carcinoma (3). Thus, we conducted a reanalysis of a scRNAseq public dataset (GSE114725) consisting of 16 primary ccRCC (13) to investigate (i) HHLA2 expression in tumor cells and (ii) CD28H expression in infiltrating NK cells. Unsupervised clustering of the dataset revealed 16 distinct clusters annotated with the genes provided in Supp Table 1, with one cluster corresponding to tumor cells, while NK cells were localized in two separate clusters (Figure 5A). Using the tumor cell signature [*CA9, KRT8, KRT18, PDK4, VEGFA, NNMT*] (13), we confirmed that some tumor cells express HHLA2 (Figure 5B) while both NK cell clusters show hight *TMIGD2* expression, which is the gene encoding CD28H (Figure 5B). Of note, HHLA2 expression was not detected in any other cluster, including in the myeloid compartment (Figure 5B). It should be

noted that we were unable to demonstrate KIR3DL3 mRNA expression on NK cells. Further subcluster analysis of the NK-1 and NK-2 clusters reveals nine distinct clusters (Figure 5C). *TMIGD2* is expressed in several of these clusters, with cluster 7 showing the highest intensity (Figure 5D, E). Differential expression analysis comparing the 9 NK clusters shows that *TMIGD2* expressing NK cells (i.e.cluster 7) also expresses genes of immature NK cells such as *KLRC1* and *NCAM1* and in constrat exhibits weak expression of mature NK genes (*B3GAT1*, *KIR3DL1*, *KIR2DL1*, *KIR2DL3)* or cytotoxic genes such as *PRF1*, *GNLY*, *GZMK*, *GZMH*, and *GZMB* (30) (Figure 5F) suggesting that tumor infiltrating NK cells which strongly express TMIGD2 are of a $CD56^{bright}$ NK cell profile (31). In conclusion, tumor-infiltrating NK cells which express high levels of *TMIGD2* exhibit a $CD56^{bright}$ phenotype with a less activated state which could be hopefully powered with an anti-CD28H agonist antibody.

Discussion

NK cell activation is controlled by the integration of signals from activating and inhibitory receptors potentially engaged by their ligands on target cells. Immunotherapies have been developed to finely tune immune cell activation against cancer cells, allowing receptor signaling even in the absence of the ligands on tumor cells. Some strategies developed to enhance NK cell functions (see (32,33) for reviews) rely on the stimulation of activating receptors such as NKp46 (34) and NKp30 (35); while others target main NK cell inhibitors like NKG2a (36) and KIRs, including KIR3DL3 (4,7). In this study, we evaluated CD28H as a potential target for immunotherapy. Indeed, given its broad distribution on NK cells (5,8) and its depicted role on T and NK cells activation (5,6), we reasoned that targeting CD28H with a mAb would increase NK cell functions and offer promising anti-tumor activity even in an HHLA2^{neg} tumor microenvironment.

We compared the ability of two anti-CD28H mAbs to initiate NK cell activation. We first showed that engagement of CD28H on NK cells induced a Ca^{2+} flux with the agonistic mAb (clone 4-5) reflecting an intracellular signaling while it did not with the blocking anti-CD28H mAb (Ab from R&D System). Hence, CD28H must be targeted at the correct epitope to activate NK cells. This observation aligns with previous findings showing that the cross-linking of activating receptors at the correct epitope influences cell activation. For instance, targeting CD38 on human NK cells with the anti-CD38 clone IB4 induced Ca^{2+} mobilization, while the anti-CD38 clone IB6 did not (37), highlighting the importance of epitope specificity in receptor activation. It has been suggested that mAbs with membrane-distal epitopes might better agonists than the eventual ligand-blocking mAbs whose epitope are closer to the membrane. However, studies evaluating different anti-CD40 (38,39) or the agonistic capacities of different anti-OX40 mAbs shatter the previously mentioned dogma. Therefore, the relationship between epitope specificity and agonistic efficacy needs to be evaluated on a case-by-case basis.

CD28H triggering activates NK cells as shown by changes in their transcriptional profile. Although fewer differentially expressed genes were observed in comparison to other studies (22,23,40), this discrepancy can be explained by the chosen kinetics and the different stimulation set-ups. Extra- and intra-cellular FACS staining further confirmed NK cell activation (i.e., 4-1BB and IFN-γ) solely after an overnight activation of CD28H. Interestingly, supernatant

from NK cells stimulated by platelet-derived growth factor D (PDGF-DD) NKp44 ligand, inhibits cancer epithelial cell lines proliferation in an IFN-γ and TNF-α dependent manner and induces CADM1 (CRTAM ligand) and CD95 (Fas) expression on these cancer cell lines (40). In our study, cell contact with target cells resulted in the secretion of IFN-γ and FAS-L by CD28H-activated NK cells. While our study focuses on hematopoietic cancer cell lines, it would also be of interest to further evaluate CD28H-triggered NK cells effector functions on human epithelial cell lines as with NKp44-activated NK cells (40). This could provide valuable insights into the potential applications of CD28H-based immunotherapy in the context of solid tumors and their interactions with tumor cells of epithelial origin.

To the best of our knowledge, our study is the first to evaluate the consequences of CD28H activation on NK cell functions by comparing different mAbs. We have demonstrated that the agonistic anti-CD28H mAb enhances NK cell cytotoxicity toward K562, DAUDI, and Jurkat target cells. No synergy was observed when CD16 and CD28H were co-engaged, as shown by both Ca^{2+} flux analysis and calcein assays ruling out synergistic effect of co-engaging CD16 and CD28H. Although Zhuang *et al.* have detected a synergy between CD28H and CD16, their assays were quite different from ours as they used the blocking anti-CD28H mAb (a mouse monoclonal Ab) and the anti-CD16 in redirected cytotoxicity assays using P815 murine target cells (also known as reverse ADCC) in which only these two molecules were engaged. A synergy was observed when co-targeting NKp46 and CD28H in Ca^{2+} flux but not in the direct cytotoxicity assay. This might be explained by the reductionist approach of the Ca^{2+} flux design experiment in which only one or two molecules are engaged. When using K562 cells, a way more complex system since target cells bring other ligands and missing/ligands essentials for NK cell activation of effector functions, the additive value of a co-engaging CD28H and NKp46 by mAbs on NK cells fades over CD28H triggering alone presumably because of target cells characteristics.

HHLA2 over-expression has been detected in various human cancers (2), including in renal cell carcinomas, where its expression is mostly found in $PDL1^{neg}$ tumor or in the rare tumor expressing both molecules, in which $HHLA2^{+}$ region is non-overlapping that of PDL1 (4). Given that HHLA2 also ligates an inhibitory receptor on T cells and on NK92-MI cells i.e. KIR3DL3 (4,7,41), we evaluated the cytotoxicity of CD28H-activated NK cells with target cells

expressing HHLA2. Our results demonstrate that HHLA2 expression on K562 target cells significantly decreases NK cell degranulation, likely due to the engagement of the inhibitory ligand KIR3DL3 as observed by others on NK92-MI cells (4,7). It is worth noting that we were not able to demonstrate KIR3DL3 expression by FACS on primary or on CD28H-activated NK cells (data not shown). However, we evidence here that CD28H-activated NK cells bypass, though not completely overcome, inhibitory signals mediated by HHLA2 or HLA-E. This observation is of particular interest for a therapeutic application of anti-CD28H mAb in clinical settings.

The percentage of CD28H-expressing NK cells is found to be lower in cancer tissues compared to the peripheral blood of patients as reported in a previous study (8) on one hand, but on the other hand, HHLA2 expression is upregulated in numerous tumor cells, thus CD28H-positive NK cells might still be activated within the tumor. Using a published scRNAseq dataset of 16 primary ccRCC (13), we show that $CD28H^{+}$ NK cells infiltrating the tumor, potentially of the $CD56^{bright}$ subtype, strongly express *CCL5* as well as *XCL1* and thus may contribute to the recruitment of cDC1 cells within the tumor site (42). These NK cells may also be responsive to mAb-based strategies targeting CD28H.

In conclusion, our study highlights that the stimulation of CD28H by a properly selected mAb enhances NK cell cytotoxicity against $HHLA2^{neg}$ target cells and bypasses inhibitory signals such as those mediated by HHLA2 and HLA-E. This finding suggests that agonistic anti-CD28H mAbs could be a promising approach for enhancing anti-tumor immune responses.

Authorship Contributions

Conceived the study: FH

Designed and supervised the experiments: PD, RL and FH

Performed experiments: PD, RL, VH, VD, BM, MD, CB, and FH

Analyzed data and/or provided samples: PD, RL, VH, VD, BM, RD, MD, CB, RJ, GB and FH

Wrote the manuscript: PD, RD and FH

Acknowledgment: This work was supported by a 2018 SANOFI iAward and the SATT. Pierre Duplouye was supported by Bpifrance in the context of a «Programme d'Investissements d'Avenir». Richard Danger was supported by the ANR project KTD-innov (ANR-17-RHUS-0010). We would like to thank Dr L. Vidard for fruitful and constructive discussions and SANOFI for the K562 HLA-A2 and K562 HLA-A2 HLA-E cells.

Conflict of Interest statement

None

References

1. Mager DL, Hunter DG, Schertzer M, Freeman JD. Endogenous Retroviruses Provide the Primary Polyadenylation Signal for Two New Human Genes (HHLA2 and HHLA3). Genomics. 1999;59(3):255–63.

2. Janakiram M, Chinai JM, Fineberg S, Fiser A, Montagna C, Medavarapu R, et al. Expression, Clinical Significance, and Receptor Identification of the Newest B7 Family Member HHLA2 Protein. Clin Cancer Res. 2015;21(10):2359–66.

3. Wang B, Ran Z, Liu M, Ou Y. Prognostic Significance of Potential Immune Checkpoint Member HHLA2 in Human Tumors: A Comprehensive Analysis. Frontiers Immunol. 2019;10:1573.

4. Bhatt RS, Berjis A, Konge JC, Mahoney KM, Klee AN, Freeman SS, et al. KIR3DL3 Is an Inhibitory Receptor for HHLA2 that Mediates an Alternative Immunoinhibitory Pathway to PD1. Cancer Immunol Res. 2021;9(2):156–69.

5. Zhu Y, Yao S, Iliopoulou BP, Han X, Augustine MM, Xu H, et al. B7-H5 costimulates human T cells via CD28H. Nat Commun. 2013;4(1):2043–2043.

6. Zhuang X, Long EO. CD28 Homolog Is a Strong Activator of Natural Killer Cells for Lysis of B7H7+ Tumor Cells. Cancer Immunol Res. 2019;7(6):939–51.

7. Wei Y, Ren X, GalboJr. PM, Moerdler S, Wang H, Sica RA, et al. KIR3DL3-HHLA2 is a human immunosuppressive pathway and a therapeutic target. Sci Immunol. 2021;6(61).

8. Crespo J, Vatan L, Maj T, Liu R, Kryczek I, Zou W. Phenotype and tissue distribution of CD28H+ immune cell subsets. Oncoimmunology. 2017;6(12):e1362529.

9. Palmer WH, Leaton LA, Codo AC, Crute B, Roest J, Zhu S, et al. Polymorphic KIR3DL3 expression modulates tissue-resident and innate-like T cells. Sci Immunol. 2023;8(84):eade5343.

10. Trundley AE, Hiby SE, Chang C, Sharkey AM, Santourlidis S, Uhrberg M, et al. Molecular characterization of KIR3DL3. Immunogenetics. 2006;57(12):904–16.

11. Ramaswamy M, Kim T, Jones DC, Ghadially H, Mahmoud TI, Garcia A, et al. Immunomodulation of T- and NK-cell Responses by a Bispecific Antibody Targeting CD28 Homolog and PD-L1. Cancer Immunol Res. 2022;10(2):200–14.

12. Zhuang X, Long EO. NK Cells Equipped With a Chimeric Antigen Receptor That Overcomes Inhibition by HLA Class I for Adoptive Transfer of CAR-NK Cells. Front Immunol. 2022;13:840844.

505 13. Alchahin AM, Mei S, Tsea I, Hirz T, Kfoury Y, Dahl D, et al. A transcriptional metastatic
506 signature predicts survival in clear cell renal cell carcinoma. Nat Commun. 2022;13(1):5747.

507 14. Kim D, Pertea G, Trapnell C, Pimentel H, Kelley R, Salzberg SL. TopHat2: accurate
508 alignment of transcriptomes in the presence of insertions, deletions and gene fusions.
509 Genome Biol. 2013;14(4):R36.

510 15. Trapnell C, Roberts A, Goff L, Pertea G, Kim D, Kelley DR, et al. Differential gene and
511 transcript expression analysis of RNA-seq experiments with TopHat and Cufflinks. Nat
512 Protoc. 2012;7(3):562–78.

513 16. Lun ATL, Chen Y, Smyth GK. It's DE-licious: A Recipe for Differential Expression Analyses
514 of RNA-seq Experiments Using Quasi-Likelihood Methods in edgeR. Methods Mol Biology
515 Clifton N J. 2016;1418:391–416.

516 17. Hochberg Y, Benjamini Y. More powerful procedures for multiple significance testing.
517 Statist Med. 1990;9(7):811–8.

518 18. Walter W, Sánchez-Cabo F, Ricote M. GOplot: an R package for visually combining
519 expression data with functional analysis. Bioinformatics. 2015;31(17):2912–4.

520 19. Vidard L, Dureuil C, Baudhuin J, Vescovi L, Durand L, Sierra V, et al. CD137 (4-1BB)
521 Engagement Fine-Tunes Synergistic IL-15– and IL-21–Driven NK Cell Proliferation. J Immunol.
522 2019;203(3):676–85.

523 20. Bryceson YT, March ME, Ljunggren HG, Long EO. Synergy among receptors on resting NK
524 cells for the activation of natural cytotoxicity and cytokine secretion. Blood.
525 2006;107(1):159–66.

526 21. Boles KS, Barchet W, Diacovo T, Cella M, Colonna M. The tumor suppressor TSLC1/NECL-
527 2 triggers NK-cell and CD8+ T-cell responses through the cell-surface receptor CRTAM. Blood.
528 2005;106(3):779–86.

529 22. Campbell AR, Regan K, Bhave N, Pattanayak A, Parihar R, Stiff AR, et al. Gene expression
530 profiling of the human natural killer cell response to Fc receptor activation: unique
531 enhancement in the presence of interleukin-12. Bmc Med Genomics. 2015;8(1):66.

532 23. Sabry M, Zubiak A, Hood SP, Simmonds P, Arellano-Ballestero H, Cournoyer E, et al.
533 Tumor- and cytokine-primed human natural killer cells exhibit distinct phenotypic and
534 transcriptional signatures. Plos One. 2019;14(6):e0218674.

535 24. Romee R, Lenvik T, Wang Y, Walcheck B, Verneris MR, Miller JS. ADAM17, a Novel
536 Metalloproteinase, Mediates CD16 and CD62L Shedding in Human NK Cells and Modulates
537 IFNγ Responses. Blood. 2011;118(21):2184–2184.

538 25. Ndhlovu LC, Lopez-Vergès S, Barbour JD, Jones RB, Jha AR, Long BR, et al. Tim-3 marks
539 human natural killer cell maturation and suppresses cell-mediated cytotoxicity. Blood.
540 2012;119(16):3734–43.

26. Zamai L, Ahmad M, Bennett IM, Azzoni L, Alnemri ES, Perussia B. Natural Killer (NK) Cell–mediated Cytotoxicity: Differential Use of TRAIL and Fas Ligand by Immature and Mature Primary Human NK Cells. J Exp Medicine. 1998;188(12):2375–80.

27. Palmer WH, Leaton LA, Codo AC, Hume PS, Crute B, Stone M, et al. Polymorphic KIR3DL3 expression modulates tissue-resident and innate-like T cells. Biorxiv. 2022;2022.08.17.503789.

28. Alter G, Malenfant JM, Altfeld M. CD107a as a functional marker for the identification of natural killer cell activity. J Immunol Methods. 2004;294(1–2):15–22.

29. Lee N, Llano M, Carretero M, Ishitani A, Navarro F, López-Botet M, et al. HLA-E is a major ligand for the natural killer inhibitory receptor CD94/NKG2A. Proc National Acad Sci. 1998;95(9):5199–204.

30. Tang F, Li J, Qi L, Liu D, Bo Y, Qin S, et al. A pan-cancer single-cell panorama of human natural killer cells. Cell. 2023;186(19):4235-4251.e20.

31. Yang C, Siebert JR, Burns R, Gerbec ZJ, Bonacci B, Rymaszewski A, et al. Heterogeneity of human bone marrow and blood natural killer cells defined by single-cell transcriptome. Nat Commun. 2019;10(1):3931.

32. Cao Y, Wang X, Jin T, Tian Y, Dai C, Widarma C, et al. Immune checkpoint molecules in natural killer cells as potential targets for cancer immunotherapy. Signal Transduct Target Ther. 2020;5(1):250.

33. Pinto S, Pahl J, Schottelius A, Carter PJ, Koch J. Reimagining antibody-dependent cellular cytotoxicity in cancer: the potential of natural killer cell engagers. Trends Immunol. 2022;43(11):932–46.

34. Gauthier L, Morel A, Anceriz N, Rossi B, Blanchard-Alvarez A, Grondin G, et al. Multifunctional Natural Killer Cell Engagers Targeting NKp46 Trigger Protective Tumor Immunity. Cell. 2019;177(7):1701-1713.e16.

35. Watkins-Yoon J, Guzman W, Oliphant A, Haserlat S, Leung A, Chottin C, et al. CTX-8573, an Innate-Cell Engager Targeting BCMA, is a Highly Potent Multispecific Antibody for the Treatment of Multiple Myeloma. Blood. 2019;134(Supplement_1):3182–3182.

36. André P, Denis C, Soulas C, Bourbon-Caillet C, Lopez J, Arnoux T, et al. Anti-NKG2A mAb Is a Checkpoint Inhibitor that Promotes Anti-tumor Immunity by Unleashing Both T and NK Cells. Cell. 2018;175(7):1731-1743.e13.

37. Mallone R, Funaro A, Zubiaur M, Baj G, Ausiello CM, Tacchetti C, et al. Signaling through CD38 induces NK cell activation. Int Immunol. 2001;13(4):397–409.

38. Yu X, Chan HTC, Orr CM, Dadas O, Booth SG, Dahal LN, et al. Complex Interplay between Epitope Specificity and Isotype Dictates the Biological Activity of Anti-human CD40 Antibodies. Cancer Cell. 2018;33(4):664-675.e4.

577 39. Zhang P, Tu GH, Wei J, Santiago P, Larrabee LR, Liao-Chan S, et al. Ligand-Blocking and
578 Membrane-Proximal Domain Targeting Anti-OX40 Antibodies Mediate Potent T Cell-
579 Stimulatory and Anti-Tumor Activity. Cell Reports. 2019;27(11):3117-3123.e5.

580 40. Barrow AD, Edeling MA, Trifonov V, Luo J, Goyal P, Bohl B, et al. Natural Killer Cells
581 Control Tumor Growth by Sensing a Growth Factor. Cell. 2018;172(3):534-548.e19.

582 41. Zhao R, Chinai JM, Buhl S, Scandiuzzi L, Ray A, Jeon H, et al. HHLA2 is a member of the B7
583 family and inhibits human CD4 and CD8 T-cell function. Proc National Acad Sci.
584 2013;110(24):9879–84.

585 42. Böttcher JP, Bonavita E, Chakravarty P, Blees H, Cabeza-Cabrerizo M, Sammicheli S, et al.
586 NK Cells Stimulate Recruitment of cDC1 into the Tumor Microenvironment Promoting
587 Cancer Immune Control. Cell. 2018;172(5):1022-1037.e14.

588

589

590

Figure 1 Triggering CD28H on NK cells with an agonistic mAb induces Ca^{2+} flux and differential gene expression. (A) Blitz analysis deciphering the CD28H/HHLA2 interaction alone, in the presence of the agonistic anti-CD28H mAb (clone 4-5) or in the presence of the anti-CD28H blocking mAb (MAB8316). The binding affinity of HHLA2 to CD28H in each condition is presented. **(B-D)** Ca^{2+} flux presented as fold increase between the BV605/PercP ratios at 20 sec and 180 sec after the cross-linking of indicated receptor combinations is presented; n=5-9 independent experiments. Non-significant differences (ns) are shown under the graph for ease of reading. **(E-G)** NK cells from 6 different HD were analyzed by bulk RNAseq after an overnight culture with the agonistic anti-CD28H mAb or the isotype control (ISO). **(E)** Volcano plot between isotype control and anti-CD28H agonistic treated groups. The 216 significantly differentially expressed genes are represented in gray circles with some gene symbols. **(F)** Significantly enriched gene ontologies (GO) related to biological processes are presented, with z-score in function of adjusted p-value calculated with the clusterProfiler and GOplot R packages, respectively. Size of the dots indicates the number of genes and colors represent 4 categories for ease of reading. **(G)** Normalized gene expression (TMM normalized cpm) in log_2 of selected genes are represented for each HD, adjusted p-value are depicted. **(H)** NK cell activation markers are presented on representative histograms of overnight stimulated NK cells with indicated culture conditions (upper panels). Geometric means of independent experiments are shown in the lower line except for 4-1BB for which percentage of positive cells is shown, each symbol represents an HD analyzed in independent experiments. **(B and H)** Significance was calculated by Wilcoxon matched pairs signed rank test **(C-D)** by a Friedmann test. ns: non-significant; *<0.05; **<0.01; ***<0.001.

Figure 2: CD28H-triggered NK cells have increased secretion functions. (A) Freshly isolated NK cells cultured overnight with depicted mAbs prior to being treated with Brefeldin A during 4h for FACS-staining of intracellular IFNγ. **(B)** Similar as in A with the respect of K562 addition during the last 4 hours of culture in the presence of Brefeldin A. **(A-B)** The percentage of IFNg positive NK cells is shown for 7 HD. Statistical analysis was performed by a Friedman test follow by a Dunn's multiple comparison test. **(C-D)** Freshly isolated NK cells cultured overnight with the depicted mAbs were then cultured for 6h with K562. NK cell secretome was analyzed by Luminex in the culture supernatants from 9 independent experiments with 9 different HD are shown. Significance was calculated by Wilcoxon matched pairs signed rank test, *<0.05; **<0.01.

Figure 3: CD28H-activated NK cells have increased direct cytotoxic activity. (A-D) NK cells, cultured overnight with indicated mAbs, were then plated for 4h in the presence of calcein labeled K562 target cells at the indicated E:T ratio (mean, ±SEM). Cytotoxicity against K562 targets cell is presented by the percentage of calcein release. n=4 to 5 independent experiments. Significance is calculated by a Two-Way Anova test followed by a Dunn's multiple comparisons test. ns: non-significant, *<0.05; **<0.01; ***<0.001; and ****<0.0001.

Figure 4: CD28H activation bypasses NK cell inhibitory signals. (A) WT (black) and HHLA2-transduced (gray) K562 cells are analyzed by FACS for their HHLA2 expression, and for their ability to bind CD28H-Fc and KIR3DL3-Fc proteins binding. **(B-C)** Freshly isolated NK cells were cultured overnight with indicated mAbs prior to being seeded with target cells at a 1:2 E:T ratio. CD107a expression was analyzed by FACS 2h00 later. **(B)** Representative FACS analysis is shown. **(C)** Percentages of CD107+ NK cells are shown for 5 independent experiments. **(D)**

HLA-E expression on HLA-A2 (black) and HLA-A2/HLA-E K562 cells (gray). **(E)** Freshly isolated NK cells were cultured overnight with indicated mAbs prior to being seeded with calcein labeled target cells at a 1:10 E:T ratio. Cytotoxicity was analyzed 4h later as calcein release; n=8 independent experiments. Significance is calculated by a Two-Way Anova test followed by a Dunn's multiple comparisons test. ns: non-significant, *<0.05; **<0.01; ***<0.001; and ****<0.0001.

Figure 5 : Single-cell RNA sequencing of primary ccRCC reveals the expression of TMIGD2 in NK cells and of HHLA2 on tumor cells. (A) UMAP visualization of all clusters (n=172 143). **(B)** UMAPs showing expression of TMIGD2 and HHLA2 in all clusters**. (C)** UMAP visualization of NK cells sub-clustering (n=28 493). **(D)** Distributions of TMIGD2 expression by the different NK clusters. **(F)** Heatmap showing the expression of corresponding genes used to define immature, mature and cytotoxic NK cells. Color indicate the gene expression.

Supplementary Figure 1: NK cell purification and activation of Ca^{2+} flux after stimulated with mAb. (A) The purity of the NK cell preparations obtained after selection is shown. **(B-D)** Fura Red-labeled NK cells were incubated with mAb against indicated receptors prior to being resuspended in HBSS 1%BSA and further analyzed by flow cytometry. BV605/PercP ratios are plotted as a function of time. The vertical dotted line represents the addition of the cross-linking mix. Representative experiments of the Figure 1 B-D are shown.

Supplementary Figure 2: Comparison of our gene signature with already published NK cell signatures. (A) The 216 significatively differentially expressed genes found in our study (Figure 1E) were compared with the gene signature published by Sabry *et al* where healthy donor NK cells were cultured either in the presence of IL-2, K562 or CTV1 cells. The Venn diagram summarizes commonly differentiated genes between each analysis. The network views summarize the network of predicted associations for a particular group of proteins. Seven differently colored lines represent the existence of the seven types of evidence used in predicting the associations. Red line indicates the presence of fusion evidence; green line

neighborhood evidence; blue line cooccurrence evidence; purple line experimental evidence; yellow line text mining evidence; light-blue line database evidence and black line co-expression evidence. **(B)** The 216 significatively differentially genes found in our study were compared with the gene signature published by Campbell *et al* in which NK cells were stimulated by IgG in the presence or not of IL-12. The Venn diagram summarizes commonly differentiated genes between each analysis. The network view summarizes the network of predicted associations for the proteins encoded by the 22 commonly up-regulated genes with our study.

Supplementary Figure 3: Secretion functions of overnight-triggered NK cells. (A-B) Luminex analysis of culture supernatants from NK cells activated overnight with the depicted mAb and then cultured for 6h with K562. n=4 independent experiment. Significance was calculated by Wilcoxon test in **(A)**, and by a Friedman test followed by a Dunn's multiple comparisons test in **(B)**; *<0.05.

Supplementary Figure 4: CD28H-activated NK cells have an increased direct cytotoxic activity. NK cells, cultured overnight with indicated mAbs, were then plated for 4h in the presence of calcein labeled target cells at indicated E:T ratios (mean, ±SEM). **(A)** Cytotoxicity against DAUDI targets, n=3. **(B)** Cytotoxicity against Jurkat targets, n=5 independent experiments. Significance is calculated by Two-Way Anova test followed by a Dunn's multiple comparisons test; ns: non-significant, *<0.05; **<0.01; ***<0.001; and ****<0.0001.

Supplementary Figure 5: HHLA2 mRNA and protein expression in different cell lines.
HHLA2 mRNA expression on different cell lines analyzed by real time quantitative PCR. HHLA2 protein expression on the same cell lines analyzed by FACS.

Supplementary Table 1 : Genes annotation

Figures

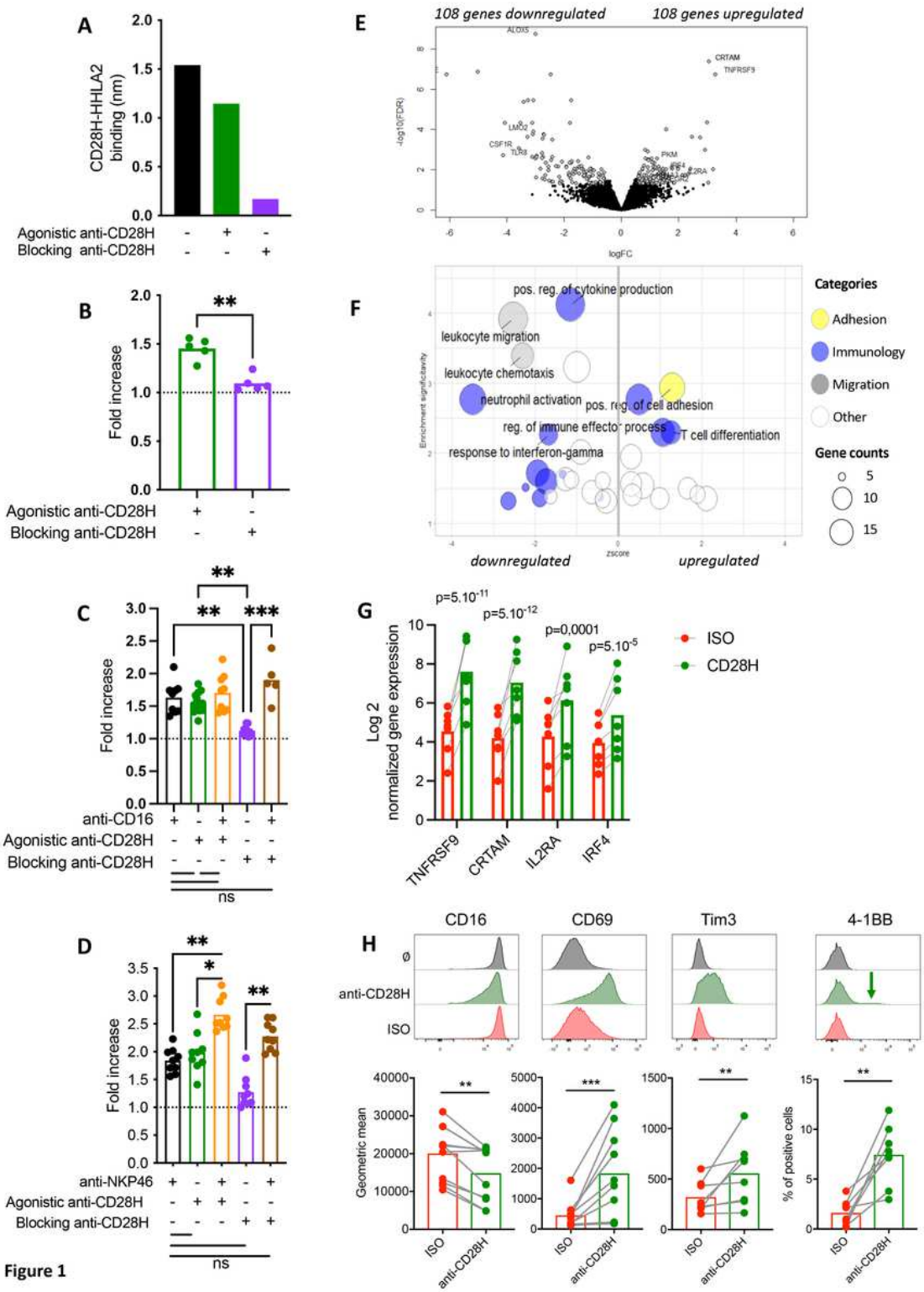

Figure 1

Triggering CD28H on NK cells with an agonistic mAb induces Ca2+ flux and differential gene expression. (A) Blitz analysis deciphering the CD28H/HHLA2 interaction alone, in the presence of the agonistic anti-CD28H mAb (clone 4-5) or in the presence of the anti-CD28H blocking mAb (MAB8316). The binding

affinity of HHLA2 to CD28H in each condition is presented. (B-D) Ca2+ flux presented as fold increase between the BV605/PercP ratios at 20 sec and 180 sec after the cross-linking of indicated receptor combinations is presented; n=5-9 independent experiments. Non-significant differences (ns) are shown under the graph for ease of reading. (E-G) NK cells from 6 different HD were analyzed by bulk RNAseq after an overnight culture with the agonistic anti-CD28H mAb or the isotype control (ISO). (E) Volcano plot between isotype control and anti-CD28H agonistic treated groups. The 216 significantly differentially expressed genes are represented in gray circles with some gene symbols. (F) Significantly enriched gene ontologies (GO) related to biological processes are presented, with z-score in function of adjusted p-value calculated with the clusterProfiler and GOplot R packages, respectively. Size of the dots indicates the number of genes and colors represent 4 categories for ease of reading. (G) Normalized gene expression (TMM normalized cpm) in log2 of selected genes are represented for each HD, adjusted p-value are depicted. (H) NK cell activation markers are presented on representative histograms of overnight stimulated NK cells with indicated culture conditions (upper panels). Geometric means of independent experiments are shown in the lower line except for 4-1BB for which percentage of positive cells is shown, each symbol represents an HD analyzed in independent experiments. (B and H) Significance was calculated by Wilcoxon matched pairs signed rank test (C-D) by a Friedmann test. ns: non-significant; * <0.05; **<0.01; ***<0.001.

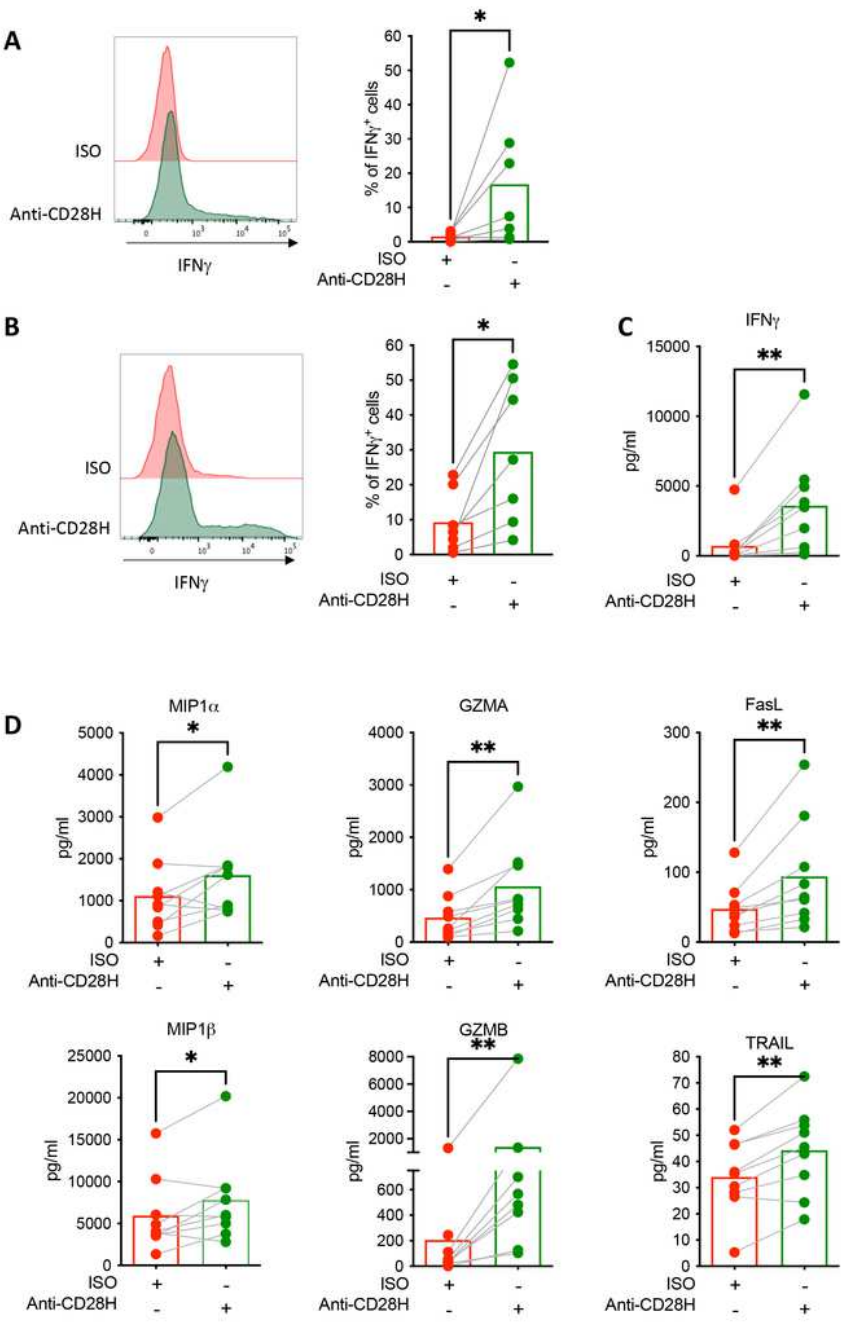

Figure 2

Figure 2

CD28H-triggered NK cells have increased secretion functions. (A) Freshly isolated NK cells cultured overnight with depicted mAbs prior to being treated with Brefeldin A during 4h for FACS-staining of intracellular IFNg. (B) Similar as in A with the respect of K562 addition during the last 4 hours of culture in the presence of Brefeldin A. (A-B) The percentage of IFNg positive NK cells is shown for 7 HD. Statistical analysis was performed by a Friedman test follow by a Dunn's multiple comparison test. (C-D) Freshly

isolated NK cells cultured overnight with the depicted mAbs were then cultured for 6h with K562. NK cell secretome was analyzed by Luminex in the culture supernatants from 9 independent experiments with 9 different HD are shown. Significance was calculated by Wilcoxon matched pairs signed rank test, *<0.05; **<0.01.

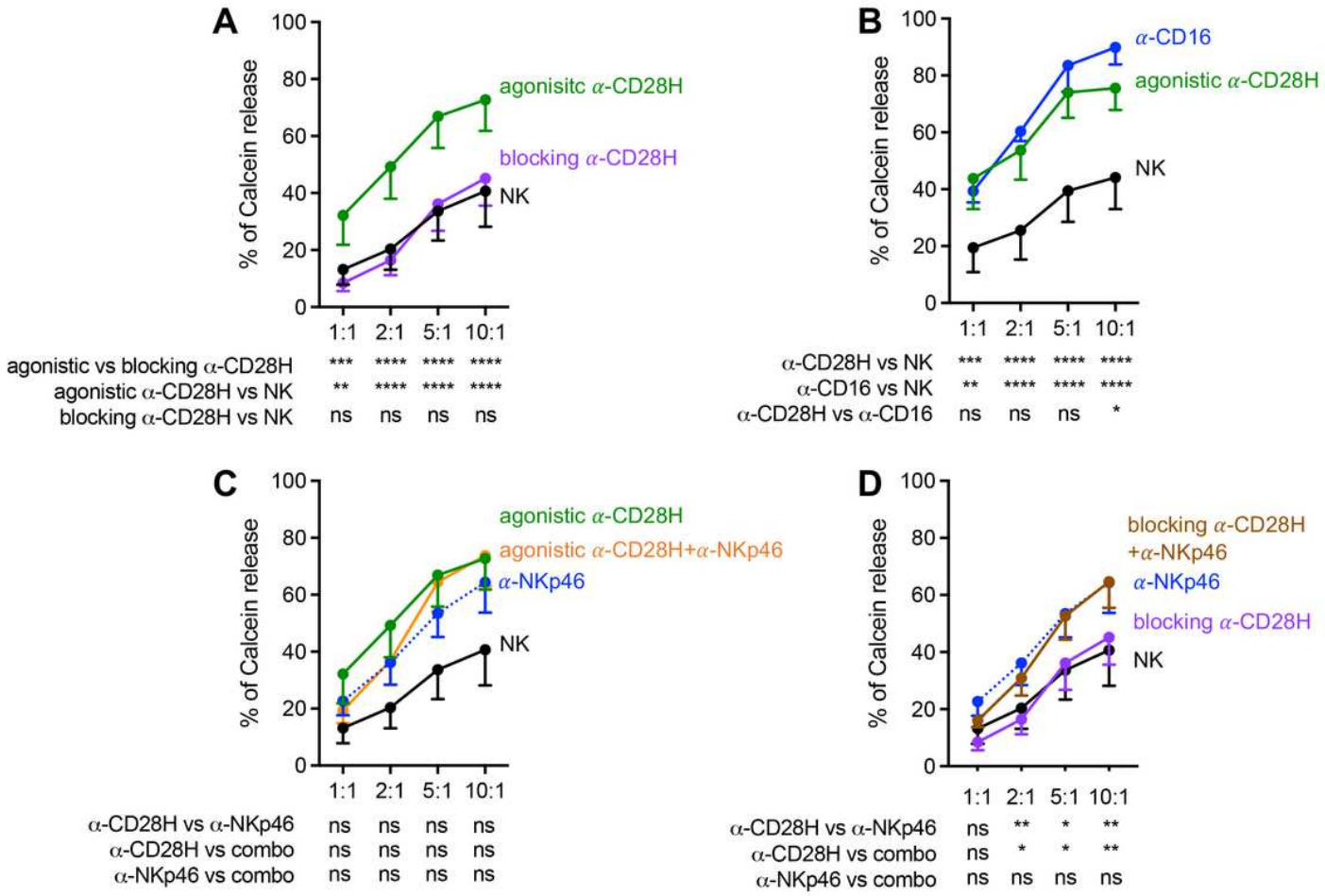

Figure 3

Figure 3

CD28H-activated NK cells have increased direct cytotoxic activity. (A-D) NK cells, cultured overnight with indicated mAbs, were then plated for 4h in the presence of calcein labeled K562 target cells at the indicated E:T ratio (mean, ±SEM). Cytotoxicity against K562 targets cell is presented by the percentage of calcein release. n=4 to 5 independent experiments. Significance is calculated by a Two-Way Anova test followed by a Dunn's multiple comparisons test. ns: non-significant, *<0.05; **<0.01; ***<0.001; and **** <0.0001.

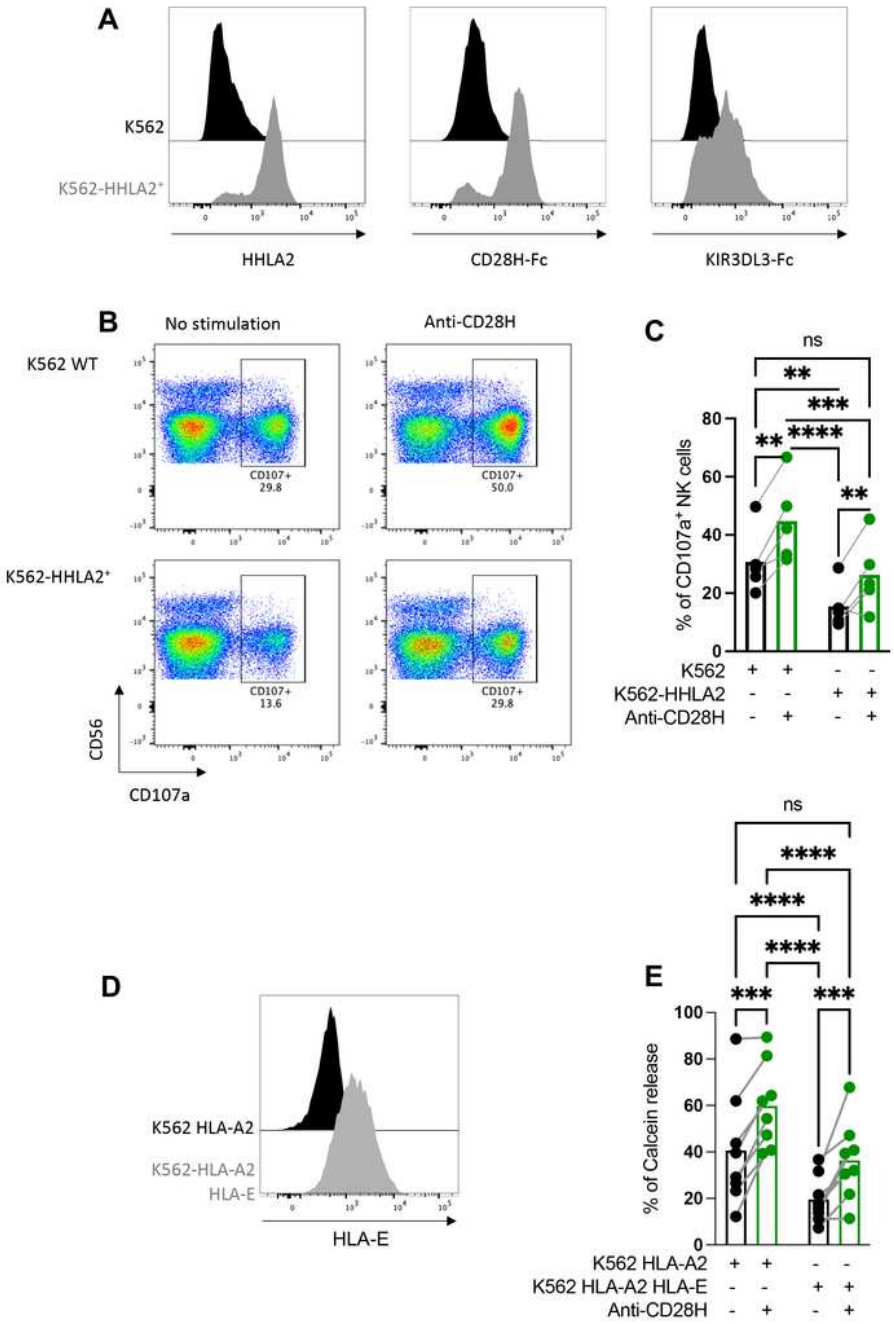

Figure 4

Figure 4

CD28H activation bypasses NK cell inhibitory signals. (A) WT (black) and HHLA2- transduced (gray) K562 cells are analyzed by FACS for their HHLA2 expression, and for their ability to bind CD28H-Fc and KIR3DL3-Fc proteins binding. (B-C) Freshly isolated NK cells were cultured overnight with indicated mAbs prior to being seeded with target cells at a 1:2 E:T ratio. CD107a expression was analyzed by FACS 2h00 later. (B) Representative FACS analysis is shown. (C) Percentages of CD107+ NK cells are shown for 5

independent experiments. (D) HLA-E expression on HLA-A2 (black) and HLA-A2/HLA-E K562 cells (gray). (E) Freshly isolated NK cells were cultured overnight with indicated mAbs prior to being seeded with calcein labeled target cells at a 1:10 E:T ratio. Cytotoxicity was analyzed 4h later as calcein release; n=8 independent experiments. Significance is calculated by a Two-Way Anova test followed by a Dunn's multiple comparisons test. ns: non-significant, *<0.05; **<0.01; ***<0.001; and ****<0.0001.

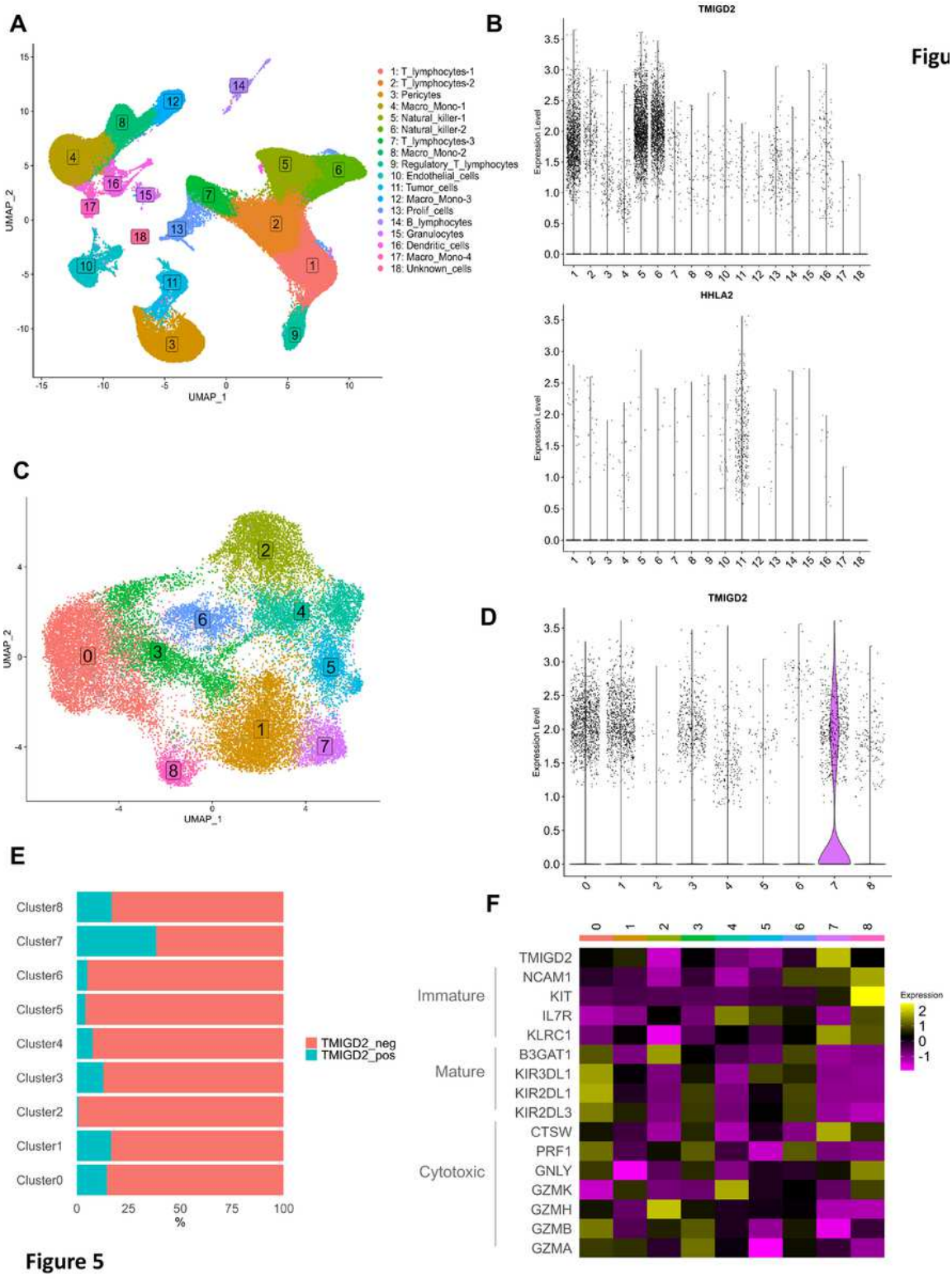

Figure 5

Figure 5

Single-cell RNA sequencing of primary ccRCC reveals the expression of TMIGD2 in NK cells and of HHLA2 on tumor cells. (A) UMAP visualization of all clusters (n=172 143). (B) UMAPs showing expression of TMIGD2 and HHLA2 in all clusters. (C) UMAP visualization of NK cells sub-clustering (n=28 493). (D) Distributions of TMIGD2 expression by the different NK clusters. (F) Heatmap showing the expression of corresponding genes used to define immature, mature and cytotoxic NK cells. Color indicate the gene expression.

Supplementary Files

This is a list of supplementary files associated with this preprint. Click to download.

- Table1.pdf
- SuppFigure1.pdf
- SuppFigure2.pdf
- SuppFigure3.pdf
- SuppFigure4.pdf
- SuppFigure5.pdf
- SuppTable1.xlsx